

Scrambling and quantum feedback in a nanomechanical system^{*}

A. K. Singh¹, Kushagra Sachan¹, L. Chotorlishvili², Vipin V.¹, and Sunil K. Mishra¹

¹ Department of Physics, Indian Institute of Technology (Banaras Hindu University), Varanasi - 221005, India

² Faculty of Mathematics and Natural Sciences, Tbilisi State University, Chavchavadze av.3, 0128 Tbilisi, Georgia

Received: date / Revised version: date

Abstract. The question of how swiftly entanglement spreads over a system has attracted vital interest. In this regard, the out-of-time ordered correlator (OTOC) is a quantitative measure of the entanglement spreading process. Particular interest concerns the propagation of quantum correlations in the lattice systems, *e.g.*, spin chains. In a seminal paper D. A. Roberts, D. Stanford and L. Susskind, *J. High Energy Phys.* **03**, 051, (2015) the concept of the OTOC's radius was introduced. The radius of the OTOC defines the front line reached by the spread of entanglement. Beyond this radius operators commute. In the present work, we propose a model of two nanomechanical systems coupled with two Nitrogen-vacancy (NV) center spins. Oscillators are coupled to each other directly while NV spins are not. Therefore, the correlation between the NV spins may arise only through the quantum feedback exerted from the first NV spin to the first oscillator and transferred from the first oscillator to the second oscillator via the direct coupling. Thus nonzero OTOC between NV spins quantifies the strength of the quantum feedback. We show that NV spins cannot exert quantum feedback on classical nonlinear oscillators. We also discuss inherently quantum case with a linear quantum harmonic oscillator indirectly coupling the two spins and verify that in the classical limit of the oscillator, the OTOC vanishes.

PACS. XX.XX.XX No PACS code given

1 Introduction

A sudden quench of parameters on the quantum state of a system leads to reshuffling of quantum information, such as the entanglement stored in a many-body correlated initial quantum state[1–9], during the subsequent time evolution. An important question is the swiftness of the spreading of the quantum entanglement. The maximum rate at which correlations buildup in the quantum system is limited by the Lieb-Robinson bound [10], while a quantitative criterion is provided by the out-of-time-ordered correlation (OTOC) of the operators in question. The concept of the OTOC was introduced by Larkin and Ovchinnikov[11], and since then, OTOC has been seen as a diagnostic tool of quantum chaos. Interest in the delocalization of quantum information (*i.e.*, the scrambling of quantum entanglement) was renewed only recently, see Refs. [12–26] and references therein. In the present work, we show that OTOC can be exploited as a quantifier of quantum feedback. In particular, we propose a model of two nanomechanical systems (nonlinear oscillators) coupled with two NV spins. We prove that entanglement between two NV centers can spread only if NV centers are connected through the quantum channel. In the semi-classical and classical channel limit, entanglement decays to zero.

Let us consider two unitary operators \hat{V} and \hat{W} , describing the local perturbations to the system, and their unitary time evolution under a Hamiltonian \hat{H} , which we will specify as, $\hat{W}(t) = \exp(i\hat{H}t) \hat{W} \exp(-i\hat{H}t)$. Here we measure time such that $\hbar = 1$. Then the OTOC is defined as

$$C(t) = \frac{1}{2} \left\langle \left[\hat{W}(t), \hat{V} \right]^\dagger \left[\hat{W}(t), \hat{V} \right] \right\rangle, \quad (1)$$

or in an equivalent form as

$$C(t) = 1 - \text{Re} \mathcal{F}(t), \quad (2)$$

where $\mathcal{F}(t) = \langle \hat{W}(t)^\dagger \hat{V}^\dagger \hat{W}(t) \hat{V} \rangle$. Here, parentheses $\langle \dots \rangle$, if not otherwise specified, denote either the quantum mechanical ground state average $\langle \dots \rangle = \langle \psi | \dots | \psi \rangle$, or the finite temperature thermal average $\langle \dots \rangle = Z^{-1} \text{Tr} \left(e^{-\beta \hat{H}} \dots \right)$ with inverse temperature $\beta = 1/T$ and the Boltzmann constant scaled to $k_B = 1$. At the initial moment of time, as follows from the definition, the OTOC is zero $C(0) = 0$, provided $[\hat{W}, \hat{V}] = 0$.

OTOCs demonstrate several interesting physical features in the integrable and nonintegrable systems. For example, magnetization OTOCs ($V = W = \text{Magnetization}$) point to dynamical phase transitions[2]. Disorder slows the growth of $C(t)$ in time, and therefore, scrambling can

be used to identify the many-body localization phase[16]. Scrambling itself is nothing other than the zero velocity Lieb Robinson bound[27].

$$C(t) = \|[W(t), V]\| = \min(|t|, 1) e^{-\eta d(\hat{W}, \hat{V})}, \quad (3)$$

Here, $\eta = \text{const}$, $d(\hat{W}, \hat{V})$ is the distance between operators on the lattice (i.e. spin operators $\exp(\hat{S}_n^z)$ of a spin chain), and the Frobenius norm of the unitary operator \hat{A} is defined as $\|\hat{A}\| = \text{Tr}(\hat{A}^\dagger \hat{A})$.

Rather interesting and enlightening is a semi-classical interpretation of scrambling. For canonical momentum and coordinate operators $V \equiv P$, $W(t) \equiv q(t)$ one deduces the equation, valid on the short time scale [12], $C(t) = \hbar^2 \exp(2\lambda_L t)$. The scrambling time is specified in terms of the classical Lyapunov exponent λ_L and is equal to the Ehrenfest time $\tau \approx \frac{1}{\lambda_L} \ln 1/\hbar$. On the other hand, a purely quantum analysis shows that the radius of the operator linearly increases in time, independent of whether the quantum system is integrable or chaotic [13]. This means that in the qubit system (for example, a Heisenberg spin chain), the time required for the formation of correlations between initially commuting operators $[\sigma_n^j, \sigma_m^k] = 2i\delta_{nm}\epsilon^{jkl}\sigma^l$ will increase linearly with the distance $d = |n - m|$ between them, and hence $[\sigma_n^j(t), \sigma_m^k] \neq 0$, for $n \neq m$. Note that customarily scrambling is an irreversible process after entanglement is spread across the system, it cannot be unscrambled[19].

Indeed OTOC can be interpreted in terms of two wave functions time evolved in a different manner. Let $|\psi(0)\rangle$ be the initial pure state wave function which is time evolved in following steps: first it is perturbed at $t = 0$ with a local unitary operator \hat{V} , then evolved forward under the unitary evolution operator $\hat{U} = \exp(-i\hat{H}t)$ until $t = \tau$, it is then perturbed at $t = \tau$ with a local unitary operator \hat{W} , and evolved backward from $t = \tau$ to $t = 2\tau$ under \hat{U}^\dagger . Hence the time evolved wave function is $|\psi(2\tau)\rangle = \hat{U}^\dagger \hat{W} \hat{U} \hat{V} |\psi(0)\rangle = \hat{W}(t) \hat{V} |\psi(0)\rangle$. For the second wave function the order of the applied perturbations is permuted, i.e. first \hat{W} at $t = \tau$ and then \hat{V} at $t = 2\tau$. Therefore the second wavefunction is $|\phi(2\tau)\rangle = \hat{V} \hat{U}^\dagger \hat{W} \hat{U} |\psi(0)\rangle = \hat{V} \hat{W}(t) |\psi(0)\rangle$ and their overlap is equivalent to the OTOC $\mathcal{F}(t) = \langle \phi(t) | \psi(t) \rangle$. What breaks the time inversion symmetry for the OTOC is the permuted sequence of operators \hat{W} and \hat{V} . Concerning the interplay between OTOC and dynamical phase transitions, we admit a recent experimental work [28]. Analyzing the behavior of the chaotic quantum system, authors experimentally observed the sudden change in the system's memory behavior.

Recently interest is focused on the hybrid quantum-classical nanoelectromechanical systems (NEMS) [29–56]. Typically a NEMS consists of two parts: quantum NV center and classical cantilever (in what follows oscillator). Therefore, NEMS may manifest binary quantum-classical features. A spin of the NV center couples with a cantilever through the magnetic tip attached to a cantilever. An oscillator performs the classical oscillations if not cooled down to the cryogenic temperatures. We are interested

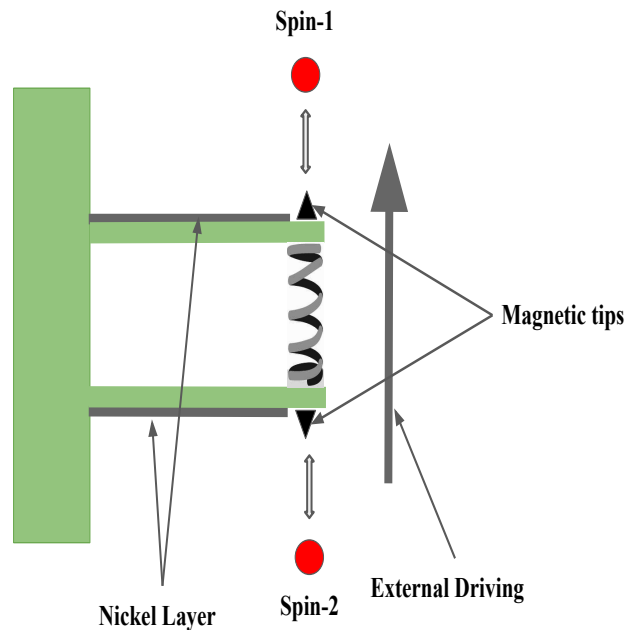


Fig. 1. (Color online) Schematics of two NV spins coupled via coupled oscillators. Oscillators are coupled to each other directly while NV spins are not.

in the question if classical coupled nonlinear oscillators may transfer the quantum correlations. In other words, we aim to explore the problem of scrambling quantum information through the classical channel. To answer this question, we study a system of two strongly coupled nonlinear NEMS. The devices consist of three layers of gallium arsenide (GaAs) the 100 nm **n**-doped layer, the 50 nm insulating layer, and the **p** doped 50 nm layer. For more details about the system we refer to the work [57]. We assume that each of the oscillators is coupled to the spin of NV center and consider OTOC as a measure of the quantum feedback. In this manuscript we will first discuss the model in section 2 and the scheme for numerical solution of the model. Afterwards, in section 3 we will discuss the analytical solution of the model in the absence of quantum feedback followed by a discussion on the numerical calculation of the system in various regimes. In section 4 we will discuss a system of two spins coupled indirectly with a quantum linear oscillator. Finally we will conclude in section 5.

2 Model

The schematics of the system in question is shown in Fig. 1. The two Oscillators are coupled to each other directly. The strength of the coupling between the oscillators depends on the coupling constant and eigenfrequencies of the oscillators. We quantify this coupling strength through the “connectivity”. The first NV spin we coupled to the first oscillator and the second NV spin to the second oscillator. On the other hand, spins are not coupled directly and

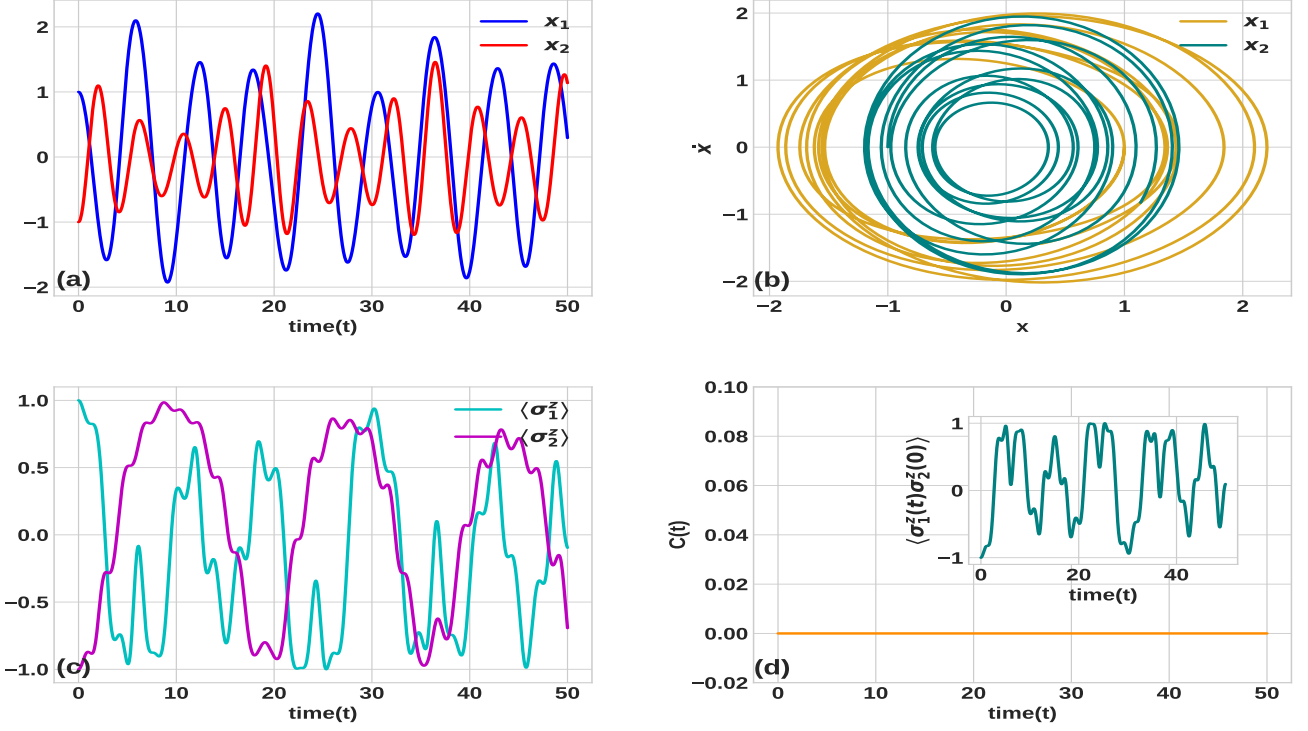


Fig. 2. Autonomous linear oscillators and weak connectivity regime: Position and phase space plots in (a) and (b), and spin dynamics and OTOC in (c) and (d). Inset in (d) shows two-point time ordered correlation. The values of the parameters are $\omega_0 = 1.5$, $\omega_1 = 1.0$, $\omega_2 = 1.5$, $F_1 = F_2 = 0$, $\xi = 0$, $\gamma = 0$, $g = 1$, $K = 0.1$, $\alpha = \pi/3$.

the correlation between NV spins may arise only through the quantum feedback exerted from the first NV spin to the first oscillator and transferred from the first oscillator to the second oscillator via the direct coupling. The Hamiltonian of the two NV spins coupled to the nonlinear oscillators reads: [58]

$$\hat{H}_s = \frac{1}{2}\omega_0(\hat{\sigma}_1^z + \hat{\sigma}_2^z) + g x_1(t)\hat{S}_1^z + g x_2(t)\hat{S}_2^z. \quad (4)$$

Here $\omega_0 = (\omega_R^2 + \delta^2)^{1/2}$, ω_R is the Rabi frequency, and δ is the detuning between the microwave frequency and the intrinsic frequency of the NV spin. The operator \hat{S}^z in the eigenbasis of the NV center has the form $\hat{S}_{1,2}^z = \frac{1}{2}(\cos \alpha \hat{\sigma}_{1,2}^z + \sin \alpha (\hat{\sigma}_{1,2}^+ + \hat{\sigma}_{1,2}^-))$, where $\hat{\sigma}^\pm = \frac{1}{2}(\hat{\sigma}_x \pm i\hat{\sigma}_y)$ and $\tan \alpha = -\omega_R/\delta$ and g is interaction constant between the oscillators and the spins. A magnetic tip is attached to the end of the nanomechanical resonators. During the oscillation performed by the resonators, the distance between the NV spin and the magnetic tip x changes. Oscillations produce a time-varying magnetic field, and therefore, the NV spin senses the motion of the magnetized resonator tip. For more details about the origin of the coupling between resonator and NV spin, we refer to the work [54]. The classical subsystem of the NEMS is the essence of two coupled non-autonomous nonlinear oscillators.

Apart from the Hamiltonian part

$$H_0 = \frac{1}{2}(\dot{x}_1^2 + \dot{x}_2^2) + \frac{1}{2}\omega_1^2 x_1^2 + \frac{1}{2}\omega_2^2 x_2^2 + \frac{1}{4}\xi x_1^4 + \frac{1}{4}\xi x_2^4 + \frac{1}{2}D(x_1 - x_2)^2, \quad (5)$$

time dependence of the oscillators $x_1(t)$, $x_2(t)$ are governed by external driving and damping terms [47, 48] and supplemented by quantum feedback term.

$$\begin{aligned} f_1 + F \cos \Omega t &= \ddot{x}_1 + \omega_1^2 x_1 + D(x_1 - x_2) + g \langle \psi | \hat{S}_1^z | \psi \rangle, \\ f_2 + F \cos \Omega t &= \ddot{x}_2 + \omega_2^2 x_2 - D(x_1 - x_2) + g \langle \psi | \hat{S}_2^z | \psi \rangle, \\ \frac{d|\psi\rangle}{dt} &= -\frac{i}{\hbar} \hat{H}_s |\psi\rangle, \\ \frac{d\langle \hat{\sigma}_{1,2}^j \rangle}{dt} &= \frac{i\omega_0}{2\hbar} \langle \psi(x_1, x_2) | [\hat{\sigma}_{1,2}^z, \hat{\sigma}_{1,2}^j] | \psi(x_1, x_2) \rangle \\ &\quad + \frac{ig}{\hbar} x_{1,2}(t) \langle \psi(x_1, x_2) | [\hat{S}_{1,2}^z, \hat{\sigma}_{1,2}^j] | \psi(x_1, x_2) \rangle. \end{aligned} \quad (6)$$

Here

$$f_{1,2} = -2\gamma \dot{x}_{1,2} - \xi x_{1,2}^3 \quad (7)$$

describes the effect of the nonlinear and damping terms on the dynamics where γ is damping constant, ξ is nonlinearity constant, F , Ω are the amplitude and frequency of the

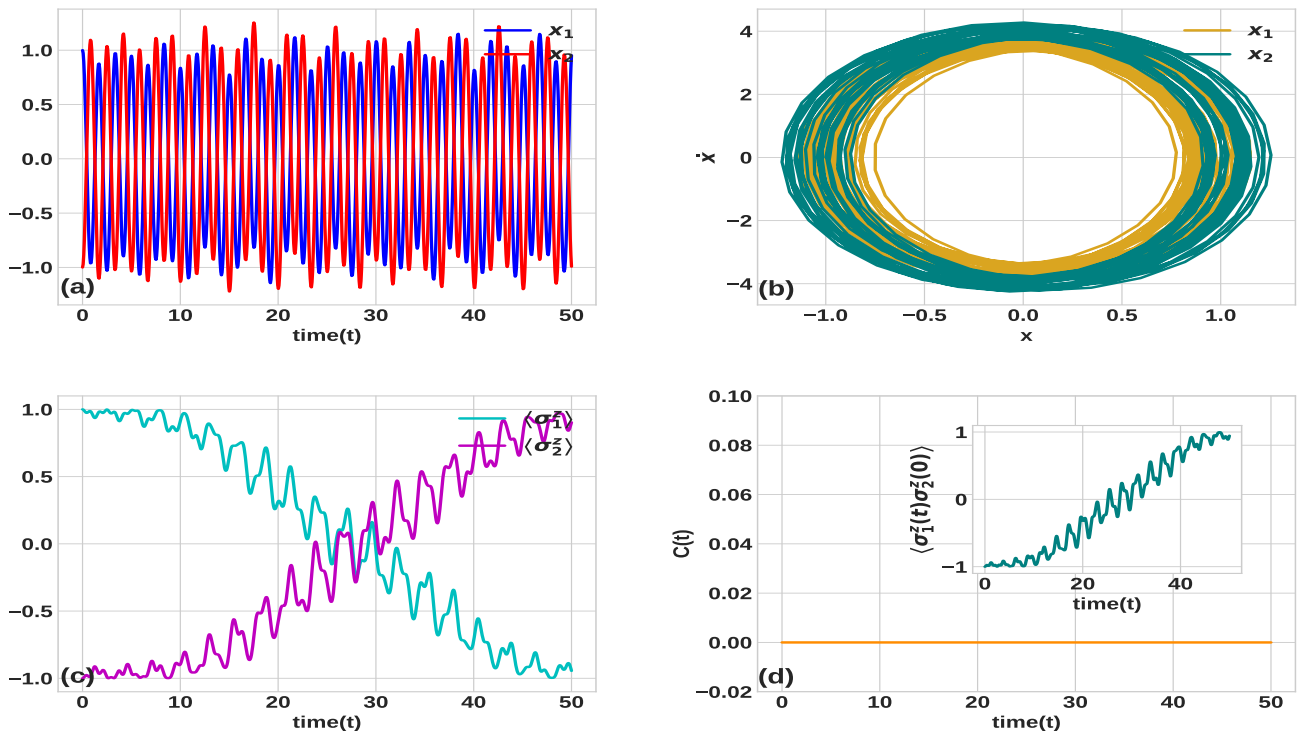


Fig. 3. Autonomous linear oscillators and strong connectivity regime: Position and phase space plots in (a) and (b), and spin dynamics and OTOC in (c) and (d). Inset in (d) shows two-point time ordered correlation. The values of the parameters are $\omega_0 = 1.5$, $\omega_1 = 1.0$, $\omega_2 = 1.5$, $F_1 = F_2 = 0$, $\xi = 0$, $\gamma = 0$, $g = 1$, $K = 10$, $\alpha = \pi/3$.

external driving and D is linear coupling term. The feedback terms $\langle \psi | \hat{S}_{1,2}^z | \psi \rangle$ describe the effect of the NV spin on the oscillator dynamics. We numerically solve the set of coupled equations Eq.(6) using Runge-Kutta Method (RK45) to integrate the wave function. The resonator is quantum if cooled down below the extremely low temperature $T < 50$ nano Kelvin [59]. Otherwise resonator performs classical oscillations and nonlinear terms are relevant when oscillation amplitude is large. Due to the feedback effect, Eq.(6) is the essence of the coupled quantum-classical dynamics. The remarkable fact is that NV spins are not coupled to each other directly but through the nonlinear classical oscillators. Later, we will also consider the inherently quantum case where the quantum case for oscillators will be considered. The coupling strength between the oscillators are quantified through the connectivity

$$K = \frac{D}{|\omega_1^2 - \omega_2^2|}. \quad (8)$$

In the case of weak connectivity, $K < 1$ oscillators perform independent oscillations, and therefore, we do not expect arise of quantum correlations between the spins. The strong connectivity $K > 1$ leads to the correlations between oscillators. Therefore, the wave function is not separable $|\psi(x_1, x_2, \hat{\sigma}_1, \hat{\sigma}_2)\rangle \neq |\psi(x_1, \hat{\sigma}_1)\rangle \otimes |\psi(x_2, \hat{\sigma}_2)\rangle$. Due to non-separability, evolved spin operators are function of the position of both the oscillators $\hat{\sigma}_{1,2}(t) \equiv \hat{\sigma}_{1,2}(x_1(t), x_2(t))$. However, correlation between the spins $[\hat{\sigma}_{1,2}(t), \hat{\sigma}_{2,1}] \neq 0$

occur only if they exert quantum feedback on the oscillators, i.e. $x_{1,2}(t, \hat{\sigma}_{1,2})$, and $\hat{\sigma}_1(x_1(t), x_2(t, \hat{\sigma}_2(t)))$. To exclude the artefacts of different dynamical regimes, we solve Eq.(6) numerically for all the possible cases of interest:

1. Autonomous linear system $F = 0$ and $f_{1,2} = 0$.
2. Autonomous nonlinear system $F = 0$, $\gamma = 0$ and $\xi \neq 0$.
3. Driven linear system $F \neq 0$, $\gamma \neq 0$ and $\xi = 0$.
4. Driven nonlinear system $F \neq 0$, $\gamma \neq 0$ and $\xi \neq 0$.

We note that Hamiltonian of the spin system Eq.(4) is coupled with the nonlinear resonator Eq.(5), [57, 60]. We explore scrambling for the weak $K \ll 1$ and strong $K > 1$ connectivity in all these cases. Taking into account the solution of the Schrödinger equation $|\psi(t)\rangle = \hat{U}(t, t_0)|\psi(t_0)\rangle$, where $\hat{U}(t, t_0) = \exp\{-i \int_{t_0}^t d\tau \hat{H}_s(\tau)\}$ is the evolution operator, we calculate $\mathcal{F} = \langle \psi(t_0) | \hat{U}^{-1} \hat{\sigma}_1^z \hat{U} \hat{\sigma}_2^z \hat{U}^{-1} \sigma_1^z \hat{U} \hat{\sigma}_2^z | \psi(t_0) \rangle$. Hereinafter, we consider the initial spin state $|\psi(t_0)\rangle = |01\rangle$ unless specified otherwise and evaluate OTOC through Eq.(2).

3 Results and discussion

3.1 Analytical solution in the absence of feedback

In the absence of quantum feedback the system admits exact analytical solution for more details see [48]. The

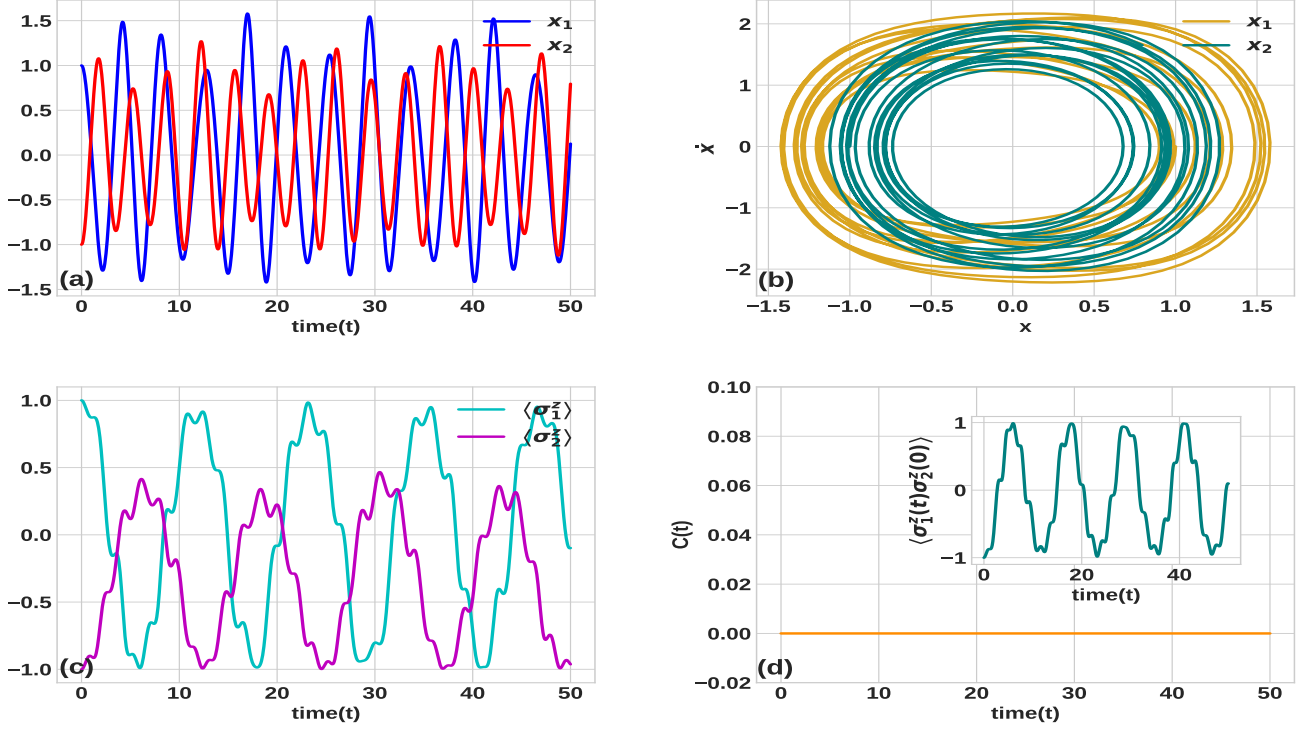


Fig. 4. Autonomous nonlinear oscillators and weak connectivity regime: Position and phase space plots in (a) and (b), and spin dynamics and OTOC in (c) and (d). Inset in (d) shows two-point time ordered correlation. The values of the parameters are $\omega_0 = 1.5$, $\omega_1 = 1.0$, $\omega_2 = 1.5$, $F_1 = F_2 = 0$, $\xi = 1$, $\gamma = 0$, $g = 1$, $K = 0.1$, $\alpha = \pi/3$.

derivation is cumbersome and we present only the final result:

$$\begin{aligned}
 x_{1,2}(t) &= \frac{F(\omega_{2,1}^2 - \Omega^2 + 2D) \cos \Omega t}{4\nu_1\nu_2\sqrt{(\nu_1 + \delta_1 - \Omega)^2 + \gamma}\sqrt{(\nu_2 + \delta_2 - \Omega)^2 + \gamma}}, \\
 \nu_{1,2} &= \omega_1^2 + \omega_2^2 + 2D \mp \frac{\omega_2^2 - \omega_1^2}{2}\sqrt{1 + K^2}, \\
 \delta_1 &= \frac{3\xi}{8}\sqrt{\frac{2}{\omega_1^2 + \omega_2^2}}(A_1^2 + A_2^2), \\
 \delta_2 &= \frac{3\xi}{8}\sqrt{\frac{2}{\omega_1^2 + \omega_2^2 + 4D}}(A_1^2 + A_2^2),
 \end{aligned} \tag{9}$$

where F , Ω are the amplitude and frequency of the external driving, D is linear coupling coefficient, $\omega_{1,2}$ are frequencies of the individual resonators, γ , ξ are damping and nonlinearity constant, $\delta_{1,2}$ are nonlinear corrections, and $A_{1,2}$ are the amplitudes of the induced resonator oscillations. We insert the solution Eq.(9) in $\hat{H}_s(x_1(t), x_2(t))$ (given by Eq. 4) and finally get the propagated wave function $|\psi(t)\rangle = \exp\left\{-i\int_{t_0}^t d\tau \hat{H}_s(\tau)\right\}|\psi(t_0)\rangle$, which is presented in the form:

$$|\psi(t)\rangle = C_1(t)|00\rangle + C_2(t)|01\rangle + C_3(t)|10\rangle + C_4(t)|11\rangle. \tag{10}$$

Here $C_1(t)$, $C_2(t)$, $C_3(t)$, $C_4(t)$ are normalisation constant and $|0\rangle, |1\rangle$ is the computational basis of NV spins. The spin dynamics reads:

$$\begin{aligned}
 \langle \hat{\sigma}_1^x \rangle &= 2\text{Re}(C_1^*(t)C_2(t) + C_3^*(t)C_4(t)), \\
 \langle \hat{\sigma}_1^y \rangle &= -2\text{Im}(C_1^*(t)C_2(t) + C_3^*(t)C_4(t)), \\
 \langle \hat{\sigma}_1^z \rangle &= (|C_1(t)|^2 + |C_3(t)|^2 - |C_2(t)|^2 - |C_4(t)|^2),
 \end{aligned} \tag{11}$$

and

$$\begin{aligned}
 \langle \hat{\sigma}_2^x \rangle &= 2\text{Re}(C_1(t)C_3^*(t) + C_2(t)C_4^*(t)), \\
 \langle \hat{\sigma}_2^y \rangle &= -2\text{Im}(C_1(t)C_3^*(t) + C_2(t)C_4^*(t)), \\
 \langle \hat{\sigma}_2^z \rangle &= (|C_1(t)|^2 + |C_2(t)|^2 - |C_3(t)|^2 - |C_4(t)|^2).
 \end{aligned} \tag{12}$$

Expressions of coefficients are cumbersome and are not presented in the explicit form.

3.2 Autonomous case

In the presence of quantum feedback we use Eq.(6) and solve the system numerically for various cases of interest. In Fig.(2), we present results obtained for the linear autonomous oscillators coupled with the weak connectivity. Dynamics of the oscillators in this case is the

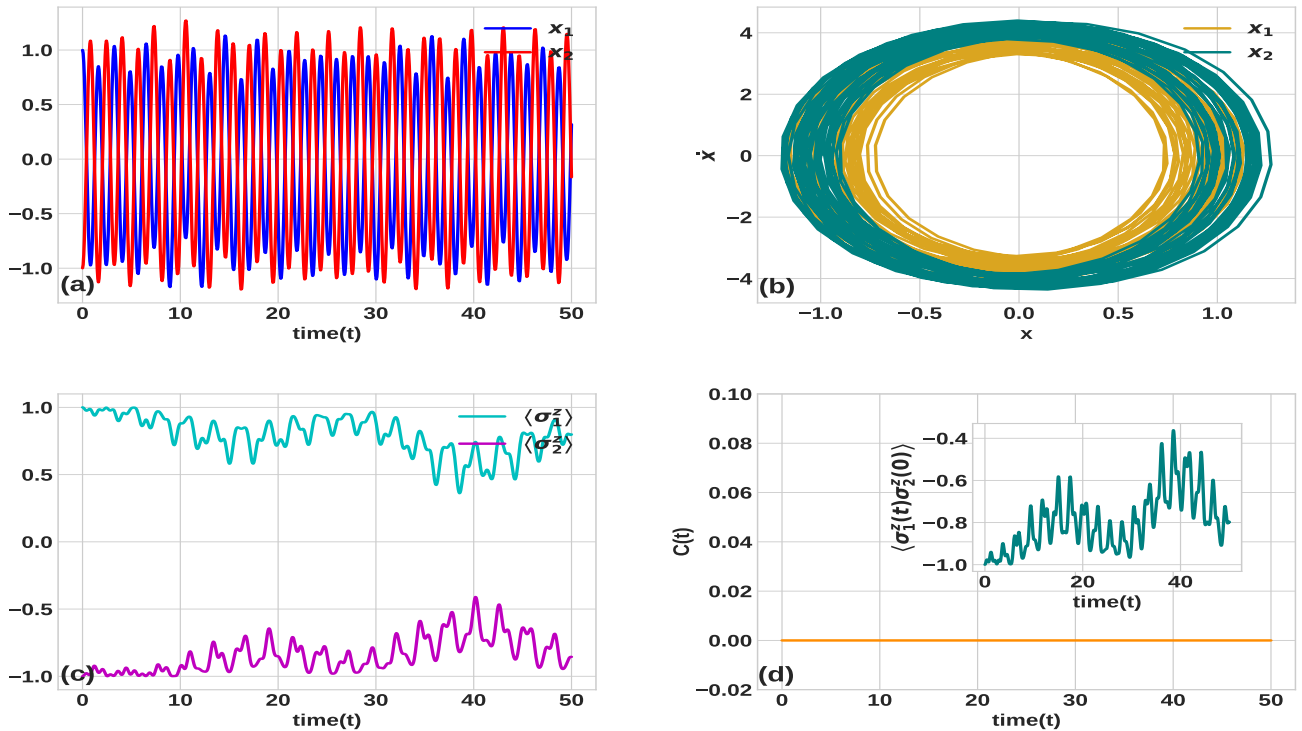


Fig. 5. Autonomous nonlinear oscillators and strong connectivity regime: Position and phase space plots in (a) and (b), and spin dynamics and OTOC in (c) and (d). Inset in (d) shows two-point time ordered correlation. The values of the parameters are $\omega_0 = 1.5$, $\omega_1 = 1.0$, $\omega_2 = 1.5$, $F_1 = F_2 = 0$, $\xi = 1$, $\gamma = 0$, $g = 1$, $K = 10$, $\alpha = \pi/3$.

essence of the harmonic oscillation with a slight modulation of amplitudes. Modulation occurs due to the exchange of energy between the oscillators. In the phase portraits (Fig.2(b)), we see the limit cycles, closed phase trajectories of periodic motion. Fig.(2)(c) describes the spin dynamics, the exchange of energy between the oscillator and the spin. We see periodic switching of the spin mediated by the weakly coupled to linear autonomous oscillators. The right-bottom plot Fig.(2)(d) shows the absence of OTOC in the system which shows a justification of the absence of quantum feedback. Two-point time ordered correlation is not zero and shows periodic switching in time (see Inset of Fig.2 (d)). In the case of strong connectivity Fig. 3 dynamics of oscillators is synchronized. The exchange of energy between the oscillators is faster leading to the trembling of the spin projection. The spin switching is slower as shown in Fig. 3 (c), and OTOC (Fig. 3(d)) is again zero. Even the strong connectivity regime could not inject the effects of quantum feedback in the system. Two-point time ordered correlation shows slow switching in this case (Inset, Fig.3 (d)).

Let us invoke the nonlinearity in the oscillators and explore the spin dynamics and quantum feedback in the system. In the beginning we consider the weak connectivity regime (see Fig. 4). As compared to the linear oscillators and the weak connectivity case, the NV spin $\hat{\sigma}_2$ coupled with the faster oscillator of position coordinate $x_2(t)$ is not switched completely. However, the NV spin

$\hat{\sigma}_1$ switches the direction completely during the course of time. Apparently, the reason is a faster change of direction of the energy flow between the spin and the oscillator. At the halfway of switching, the energy starts to flow back to the oscillator. The quantum feedback is absent in this case also (see Fig. 4 (d)). We see in (Fig.4 (d)) inset that time ordering two point correlation shows oscillations in time with a frequency smaller than the linear case.

Next, we explore spin dynamics and quantum feedback in the case of strongly coupled nonlinear oscillators as shown in Fig.(5). We see that NV spins are frozen and perform small trembling oscillations in the vicinity of the initial values (Fig.5 (c)). The quantum feedback quantified in terms of OTOC (Fig.5 (d)) is again zero in this dynamical regime. We see in inset (Fig.5 (d)) that two-point time ordered correlation shows oscillations with the peak increasing in time. The nonlinearity deters the switching of the two-point time ordered correlation in the given observation.

3.3 External driving

We know that the forced oscillations are the essence of two different evolution steps. At the early stage, the oscillation frequency coincides with the eigenfrequency of the system. However, after a specific time, the system switches to the frequency of the driving force. At first we consider the weak connectivity regime. During the transition step, we

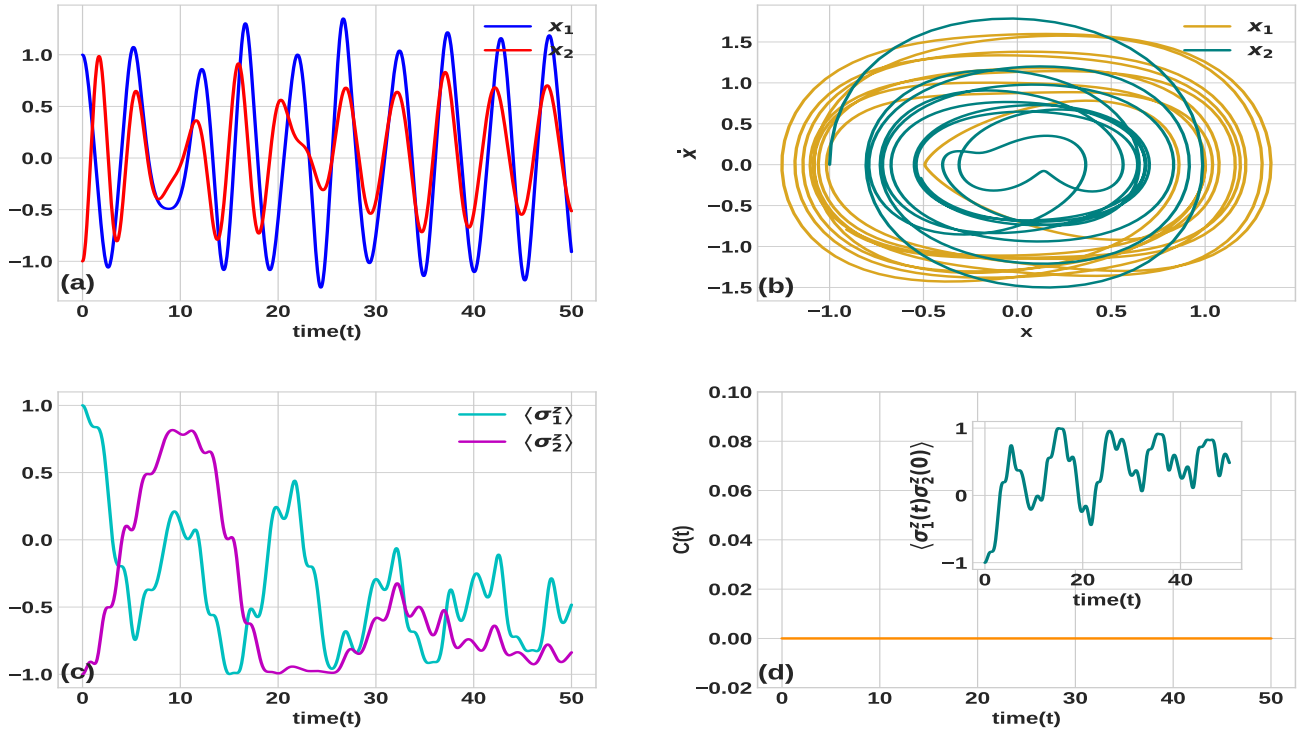


Fig. 6. Driven nonlinear oscillators and weak connectivity regime: Position and phase space plots in (a) and (b), and spin dynamics and OTOC in (c) and (d). Inset in (d) shows two-point time ordered correlation. The values of the parameters are $\omega_0 = 1.5$, $\omega_1 = 1.0$, $\omega_2 = 1.5$, $F_1 = F_2 = 0.5$, $\xi = 1$, $\gamma = 0.15$, $g = 1$, $K = 0.1$, $\alpha = \pi/3$.

observe switching of the NV spins Fig.(6)(c). However, after reaching in the forced oscillation regime, the NV spins are frozen. We note that the amplitude of oscillations does not increase resonantly due to the nonlinearity destroying the nonlinear resonance. In the case of a strong connectivity (see Fig.7), oscillators are well synchronized. The NV spins and oscillator mode periodically exchange energy. In both the cases of weak and strong connectivity, OTOC and quantum feedback are absent. We see in inset of Fig.6 (d) and Fig.7 (d) that two-point time ordered correlation is not zero shows switching.

In order to explain the absence of the quantum feedback and scrambling in the strong connectivity case, we plot the energies of classical oscillators and the quantum NV spin system. We neglect the coupling with the external driving field and dissipation process to analyse the autonomous system. In this case, the total energy of the system comprising the NV spins and the oscillator is conserved. As we see Fig.(8) (a) and (b), the ratio between energies $\langle H_{NV} \rangle / H_0 = 0.02$ is rather small, meaning that the energy of the oscillator is much larger than the energy of the spin system. The interaction between the oscillators and spins strongly affects NV spins and only slightly affects the oscillators. Another argument is that the relative modulation depth of energies is much larger for the quantum system: $\delta H_0 / H_0 \approx 0.1$, $\delta \langle H_{NV} \rangle / \langle H_{NV} \rangle \approx 3$ and $\delta H_0 + \delta \langle V \rangle + \delta \langle H_{NV} \rangle = 0$. This argument becomes even stronger when external driving is switched on. The

external driving field supplies the energy to the oscillators and smears out the quantum feedback effect. OTOC has also been calculated for the initial state $|\psi(t_0)\rangle = \frac{1}{\sqrt{2}}(|01\rangle - |10\rangle)$. It turned out to be zero even for the Bell states, however, the entanglement is preserved during the process.

4 Inherently quantum case: Non-zero OTOC, geometric measure of entanglement and concurrence

In the case of strong connectivity, to some extent, coupled oscillators physically are the essence of a single effective oscillator. We show that the effective oscillator interacting with both spins indirectly couples spins. We study three measures of quantum correlations: OTOC, concurrence, and a geometric measure of entanglement [61–63]. We consider Bell’s state as an initial state of the system and show that concurrence and a geometric measure of entanglement do not capture the effect of the quantum feedback. On the other hand, OTOC precisely quantifies the effect of quantum feedback. However, this effect disappears in the classical limit. Before proceed further, once

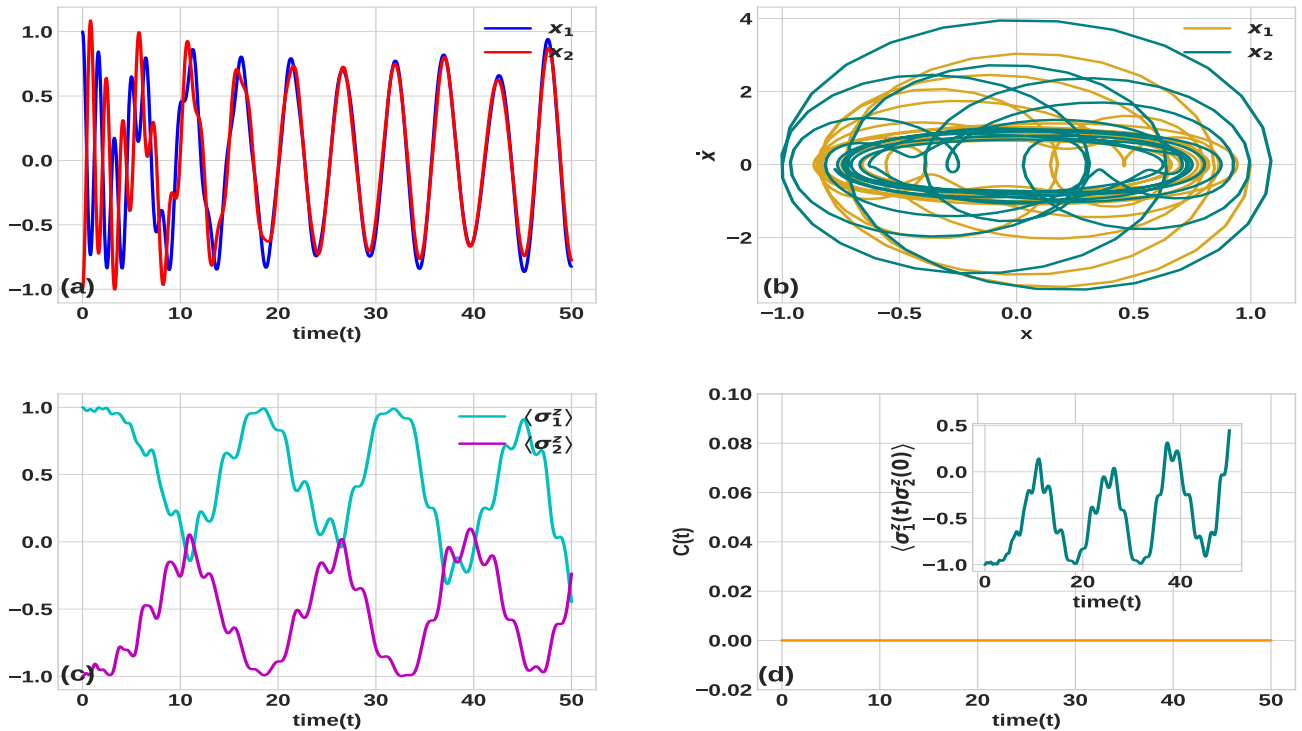


Fig. 7. Driven nonlinear oscillators and strong connectivity regime: Position and phase space plots in (a) and (b), and spin dynamics and OTOC in (c) and (d). Inset in (d) shows two-point time ordered correlation. The values of the parameters are $\omega_0 = 1.5$, $\omega_1 = 1.0$, $\omega_2 = 1.5$, $F_1 = F_2 = 0.5$, $\xi = 1$, $\gamma = 0.15$, $g = 1$, $K = 10$, $\alpha = \pi/3$.

again, we specify the Hamiltonian of the system.

$$\begin{aligned} \hat{H} &= \hat{H}_0 + g\hat{V}, \\ \hat{H}_0 &= \omega_0 (\hat{\sigma}_1^z + \hat{\sigma}_2^z) + \omega \hat{a}^+ \hat{a}, \\ \hat{V} &= \{\hat{a}^+ (\hat{\sigma}_1^- + \hat{\sigma}_2^-) + \hat{a} (\hat{\sigma}_1^+ + \hat{\sigma}_2^+)\}. \end{aligned} \quad (13)$$

Here ω_0 is the frequency of NV spin, ω is the frequency of oscillator and g is NV spin-oscillator coupling constant. For the sake of simplicity we limit the discussion of the quantum case to the linear system only. We note that inclusion of nonlinear terms leads to the dynamical Stark shift $(\omega_0 + \xi \hat{a}^+ \hat{a}) \hat{\sigma}_{1,2}$ and two-photon processes $\hat{\sigma}_{1,2}^+ \hat{a}^2$, $\hat{\sigma}_{1,2}^- (\hat{a}^+)^2$, see [43] for more details. Nonlinear terms may affect results only quantitatively.

We follow the Fröhlich method [64] and consider transformation of the Hamiltonian $\tilde{H} = \exp(-\hat{S}) \hat{H} \exp(\hat{S})$, where operator \hat{S} satisfies the condition $g\hat{V} + [\hat{H}_0, \hat{S}] = 0$ and ensures the absence of the linear non-diagonal terms proportional to g term in the transformed Hamiltonian [64]. Hamiltonian of effective interaction between two NV spins mediated by linear quantum cantilever can be derived as follows [59]:

$$\begin{aligned} \hat{H}_{eff} &= \frac{ig^2}{2} \int_{-\infty}^0 d\tau \left[\hat{V}(\tau), V(0) \right], \\ \hat{V}(t) &= \exp(-i\hat{H}_0 t) \hat{V} \exp(i\hat{H}_0 t). \end{aligned} \quad (14)$$

Taking into account Eq.(13) and Eq.(14) we deduce:

$$\begin{aligned} \hat{H}_{eff} &= \frac{g^2 (2\hat{a}^+ a + 1)}{\omega_0 - \omega} \times \\ &\left\{ (\hat{\sigma}_1^z + \hat{\sigma}_2^z) + \frac{\hat{\sigma}_1^+ \hat{\sigma}_2^- + \hat{\sigma}_1^- \hat{\sigma}_2^+}{(2\hat{a}^+ a + 1)} \right\}. \end{aligned} \quad (15)$$

The total Hamiltonian has the form:

$$\hat{H}_{tot} = \hat{H}_0 + \hat{H}_{eff}. \quad (16)$$

In what follows we replace $n = \langle \hat{a}^+ a \rangle$ and rescale the total Hamiltonian $\hat{H}_{tot} / (2n + 1)$. In case of local unitary and Hermitian Pauli matrices the following expression of OTOC can be deduced from Eq. (2):

$$C(t) = 1 - \text{Re} \left[\langle \hat{\sigma}_1^z(t) \hat{\sigma}_2^z \hat{\sigma}_1^z(t) \hat{\sigma}_2^z \rangle \right] \quad (17)$$

where time dependence is governed by total Hamiltonian as $\hat{\sigma}_1^z(t) = e^{-it\hat{H}_{tot}} \hat{\sigma}_1^z e^{it\hat{H}_{tot}}$. Taking into account Eq.(16) and the initial Bell's state $|\Phi^-\rangle = 1/\sqrt{2}(|01\rangle - |10\rangle)$ (which is also an eigenstate of the system), for OTOC from Eq.(17) we deduce:

$$C(t) = 2 \sin^2(4\Omega_n t), \quad (18)$$

where $\Omega_n = \frac{g^2}{(\omega_0 - \omega)(2n + 1)}$. As we see from Eq.(18), in the initial moment of time OTOC is zero $C(t = 0) = 0$ and becomes non zero for $t > 0$. However in the semi-classical

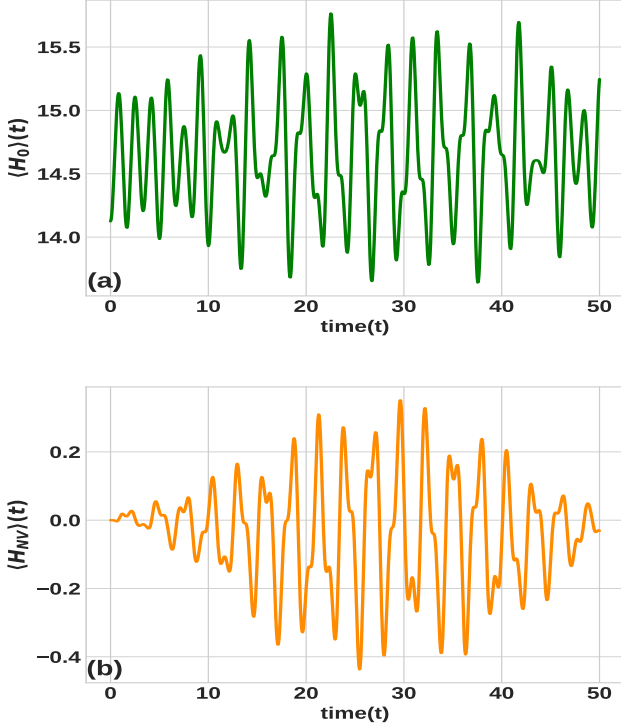


Fig. 8. Plot of average energy versus time for (a) the oscillator and (b) the NV spin, in the strong connectivity regime. The values of the parameters are: $\omega_0 = 1.5$, $\omega_1 = 1.0$, $\omega_2 = 1.5$, $F_1 = F_2 = 0$, $\xi = 0$, $\gamma = 0$, $g = 1$, $K = 10$, $\alpha = \pi/3$. The modulation depth of energies $\delta\langle H_{NV} \rangle = 0.5$, $\delta H_0 = 1.5$

limit $n \rightarrow \infty$, $\Omega_n \rightarrow 0$ and to detect effect of the quantum feedback we need to wait rather long time $t \approx 1/\Omega_n$, meaning that effect of the quantum feedback is rather weak (zero).

For a two-qubit system geometric measure of entanglement (GME) and concurrence are related to each other [62]. To calculate concurrence we follow standard recipes:

$$\mathcal{C}[t] = \max(0, R_1 - R_2 - R_3 - R_4), \quad (19)$$

where $R_n(t)$ are the square roots from the eigenvalues of the following matrix

$$\hat{R}(t) = \hat{\rho}_R(t) (\hat{\sigma}_1^y \otimes \hat{\sigma}_2^y) \hat{\rho}_R^*(t) (\hat{\sigma}_1^y \otimes \hat{\sigma}_2^y), \quad (20)$$

$\hat{\rho}_R(t) = \text{Tr}_{field}(\hat{\rho}(t))$ is the reduced density matrix $\hat{\rho}(t) = e^{-it\hat{H}_{tot}}\hat{\rho}(0)e^{it\hat{H}_{tot}}$, $\hat{\rho}(0) = |\Phi^-\rangle\langle\Phi^-|$ and $\hat{\sigma}_{1,2}^y$ are Pauli matrices acting on the first and the second spins. The GME is given by $\text{GME} = (1 - \sqrt{1 - \mathcal{C}[t]})/2$ [62]. For the Hamiltonian Eq.(16) and the initial Bell's state $|\Phi^-\rangle = 1/\sqrt{2}(|01\rangle - |10\rangle)$, we calculate $\mathcal{C}[t] = 1$ and $\text{GME} = 0.5$. Thus in the case of a particular initial state, the concurrence and GME are constant, and through them, we cannot quantify quantum feedback exerted by spins on the oscillator. On the other hand, the quantum feedback if described by OTOC, will be nonzero if present (as in quantum case) and vanish if absent (as in the classical

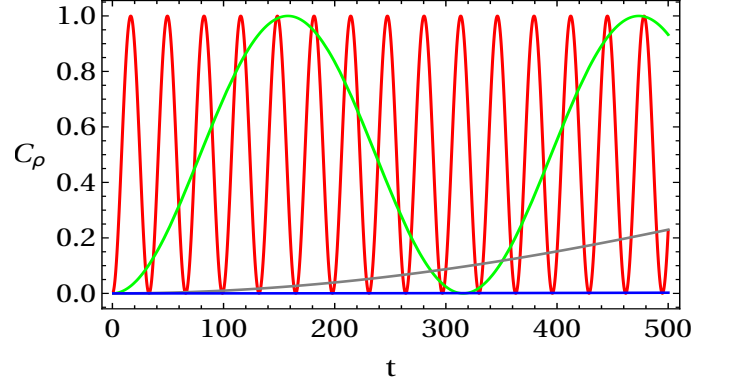


Fig. 9. Plot of thermally averaged OTOC vs time at fixed Temperature(T). The parameters used are $g = 1$, $\omega_0 = 3$, $\omega = 2$, $T = 100$, $n = 10$ (red), $n = 100$ (Green), $n = 1000$ (Gray), $n = 10000$ (blue). For very large n the oscillations die out.

limit). We can also check the finite temperature case. At a finite temperature, in the equilibrium state, the density matrix in the basis of Hamiltonian is given as

$$\hat{\rho} = Z^{-1} \begin{pmatrix} e^{-2\beta(\Omega_0 + \omega_{0R})} & 0 & 0 & 0 \\ 0 & e^{-\beta\Omega_n} & 0 & 0 \\ 0 & 0 & e^{\beta\Omega_n} & 0 \\ 0 & 0 & 0 & e^{2\beta(\Omega_0 + \omega_{0R})} \end{pmatrix}, \quad (21)$$

$$Z = 2 \cosh \beta 2(\Omega_0 + \omega_{0R}) + 2 \cosh \beta \Omega_n,$$

where we introduced the notations $\Omega_0 = \frac{g^2}{2n+1}$, $\omega_{0R} = \frac{\omega_0}{2n+1}$ and $\beta = 1/T$ is the inverse temperature. Thermally averaged OTOC $C_\rho = 1 - \text{Re}(\text{Tr}\{\hat{\rho}\hat{\sigma}_1^z(t)\hat{\sigma}_2^z\hat{\sigma}_1^z(t)\hat{\sigma}_2^z\})$ is calculated (for details see Appendix A) as:

$$C_\rho = 1 - \frac{\cosh 2\beta(\Omega_0 + \omega_{0R}) + \cos 4\Omega_n t \cosh \beta \Omega_n}{\cosh 2\beta(\Omega_0 + \omega_{0R}) + \cosh \beta \Omega_n}, \quad (22)$$

and the thermal concurrence $\mathcal{C}_\rho[t]$ is calculated using Eq. (19) as

$$\mathcal{C}_\rho[t] = 2 \times \max\left(0, \frac{|\sinh \beta \Omega_n| - 1}{(2 \cosh 2\beta(\Omega_0 + \omega_{0R}) + 2 \cosh \beta \Omega_n)}\right). \quad (23)$$

Thermally averaged OTOC as a function of time is plotted in Fig.(9) for different n . At the finite temperatures, in the semi-classical limit $n \rightarrow \infty$, we have $\Omega_n \rightarrow 0$, $\omega_{0R} \rightarrow 0$, $C_\rho = 0$ and $\mathcal{C}_\rho[t] = 0$. On the other hand, at a zero temperature dynamical effect, i.e., the quantum feedback is captured only by OTOC. Both at finite or zero temperature OTOC is not zero if spin exerts feedback on the oscillator, and it becomes zero when $n \rightarrow \infty$.

5 Conclusions

Out of time correlation function is widely used as a quantitative measure of spreading quantum correlations. In the

present work, we propose an experimentally feasible model of the nanomechanical system for which OTOC can be exploited as a quantifier of quantum feedback. In particular, we consider two NV spins coupled with two different oscillators. Oscillators are coupled to each other directly, and NV spins are not. Therefore, any quantum correlation between the NV spins may arise only due to the quantum feedback exerted by NV spins on the corresponding oscillators. The OTOC operator between the NV spins is the essence of the quantifier of the quantum feedback. To exclude the artefacts of a particular type of oscillations, we considered different dynamical regimes: linear vs. non-linear, free, and forced oscillations and showed that the OTOC and quantum feedback are zero in all the cases. We also considered quantum oscillator and quantum spins case where the indirect coupling between the spins is invoked by a quantum harmonic oscillator. We have shown nonzero OTOC, GME and concurrence in this case. In a classical limit of the oscillator, the OTOC vanishes. Thus, we conclude that entanglement between two NV centers can spread only if NV centers are connected through the quantum channel. In the semi-classical and classical channel limit, entanglement decays to zero.

A Appendix: Calculation of thermally averaged OTOC C_ρ

From Eq.(16) after re-scaling the total Hamiltonian will be written as:

$$H_{tot} = (\omega_{0R} + \Omega_0)(\sigma_1^z + \sigma_2^z) + \Omega_n(\sigma_1^+ \sigma_2^- + \sigma_1^- \sigma_2^+) \quad (24)$$

or in the matrix form, in the standard basis,

$$\begin{pmatrix} 2(\Omega_0 + \omega_{0R}) & 0 & 0 & 0 \\ 0 & 0 & \Omega_n & 0 \\ 0 & \Omega_n & 0 & 0 \\ 0 & 0 & 0 & -2(\Omega_0 + \omega_{0R}) \end{pmatrix}, \quad (25)$$

where $n = \langle a^\dagger a \rangle$, $\omega_{0R} = \frac{\omega_0}{2n+1}$, and $\Omega_0 = \frac{g^2}{\omega_0 - \omega}$, and $\Omega_n = \frac{g^2}{(\omega_0 - \omega)(2n+1)}$. The eigenstates of the above Hamiltonian are

$$|\phi_1\rangle = |0, 0\rangle, \quad (26)$$

$$|\phi_2\rangle = \frac{1}{\sqrt{2}}(|1, 0\rangle + |0, 1\rangle), \quad (27)$$

$$|\phi_3\rangle = \frac{1}{\sqrt{2}}(|1, 0\rangle - |0, 1\rangle), \quad (28)$$

$$|\phi_4\rangle = |1, 1\rangle, \quad (29)$$

with corresponding eigenvalues:

$$E_1 = 2(\Omega_0 + \omega_{0R}) \quad (30)$$

$$E_2 = \Omega_n \quad (31)$$

$$E_3 = -\Omega_n \quad (32)$$

$$E_4 = -2(\Omega_0 + \omega_{0R}). \quad (33)$$

At a finite temperature, in the equilibrium state the density matrix $\hat{\rho} = Z^{-1}e^{-\beta H_{tot}}$ of the system in the diagonal basis of the Hamiltonian is

$$\hat{\rho} = Z^{-1}(e^{-\beta E_1}|\phi_1\rangle\langle\phi_1| + e^{-\beta E_2}|\phi_2\rangle\langle\phi_2| + e^{-\beta E_3}|\phi_3\rangle\langle\phi_3| + e^{-\beta E_4}|\phi_4\rangle\langle\phi_4|) \quad (34)$$

$$\hat{\rho} = Z^{-1} \begin{pmatrix} e^{-2\beta(\Omega_0 + \omega_{0R})} & 0 & 0 & 0 \\ 0 & e^{-\beta\Omega_n} & 0 & 0 \\ 0 & 0 & e^{\beta\Omega_n} & 0 \\ 0 & 0 & 0 & e^{2\beta(\Omega_0 + \omega_{0R})} \end{pmatrix}, \quad (35)$$

$$Z = 2 \cosh \beta 2(\Omega_0 + \omega_{0R}) + 2 \cosh \beta \Omega_n.$$

Pauli operators σ_1^z and σ_2^z in the diagonal basis of Hamiltonian are written as:

$$\sigma_1^z = |\phi_1\rangle\langle\phi_1| + |\phi_3\rangle\langle\phi_3| + |\phi_2\rangle\langle\phi_2| - |\phi_4\rangle\langle\phi_4| \quad (36)$$

$$\sigma_2^z = |\phi_1\rangle\langle\phi_1| - |\phi_3\rangle\langle\phi_3| - |\phi_2\rangle\langle\phi_2| - |\phi_4\rangle\langle\phi_4| \quad (37)$$

Also the time evolution operators $\exp(-iH_{tot}t)$ in the diagonal basis can be given as:

$$\exp(-iH_{tot}t) = e^{-iE_1 t}|\phi_1\rangle\langle\phi_1| + e^{-iE_2 t}|\phi_2\rangle\langle\phi_2| + e^{-iE_3 t}|\phi_3\rangle\langle\phi_3| + e^{-iE_4 t}|\phi_4\rangle\langle\phi_4|, \quad (38)$$

We calculate $\sigma_1^z(t)$ as

$$\sigma_1^z(t) = e^{iH_{tot}t}\sigma_1^z e^{-iH_{tot}t} = |\phi_1\rangle\langle\phi_1| + e^{-2i\Omega_n t}|\phi_3\rangle\langle\phi_3| + e^{2i\Omega_n t}|\phi_2\rangle\langle\phi_2| - |\phi_4\rangle\langle\phi_4|. \quad (39)$$

By successive application of operators in the sequence $\sigma_1^z(t)\sigma_2^z\sigma_1^z(t)\sigma_2^z$ we get:

$$\sigma_1^z(t)\sigma_2^z\sigma_1^z(t)\sigma_2^z = (|\phi_1\rangle\langle\phi_1| - e^{4i\Omega_n t}|\phi_2\rangle\langle\phi_2| - e^{-4i\Omega_n t}|\phi_3\rangle\langle\phi_3| + |\phi_4\rangle\langle\phi_4|). \quad (40)$$

We can calculate $\rho\sigma_1^z(t)\sigma_2^z\sigma_1^z(t)\sigma_2^z$ as

$$\rho\sigma_1^z(t)\sigma_2^z\sigma_1^z(t)\sigma_2^z = Z^{-1}(e^{-2\beta(\Omega_0 + \omega_{0R})}|\phi_1\rangle\langle\phi_1| - e^{-\beta\Omega_n}e^{4i\Omega_n t}|\phi_2\rangle\langle\phi_2| - e^{\beta\Omega_n}e^{-4i\Omega_n t}|\phi_3\rangle\langle\phi_3| + e^{2\beta(\Omega_0 + \omega_{0R})}|\phi_4\rangle\langle\phi_4|). \quad (41)$$

Further, we calculate the thermally averaged OTOC $C_\rho(t) = 1 - \text{Re}(\text{Tr}\{\rho\sigma_1^z(t)\sigma_2^z\sigma_1^z(t)\sigma_2^z\})$ as

$$C_\rho(t) = 1 - \frac{2 \cosh 2\beta(\Omega_0 + \omega_{0R}) + 2 \cos 4\Omega_n t \cosh \beta \Omega_n}{Z}, \quad (42)$$

Author contribution statement

AKS, LC and SKM conceived of the presented idea and developed the theory and performed analysis. AKS, KS and VV performed numerical calculations. All authors discussed the results and contributed to the final manuscript.

References

1. Markus Heyl. Dynamical quantum phase transitions: a review. *Reports on Progress in Physics*, 81(5):054001, apr 2018.
2. Markus Heyl, Frank Pollmann, and Balázs Dóra. Detecting equilibrium and dynamical quantum phase transitions in ising chains via out-of-time-ordered correlators. *Phys. Rev. Lett.*, 121:016801, Jul 2018.
3. M. Heyl, A. Polkovnikov, and S. Kehrein. Dynamical quantum phase transitions in the transverse-field ising model. *Phys. Rev. Lett.*, 110:135704, Mar 2013.
4. Ronen Vosk and Ehud Altman. Dynamical quantum phase transitions in random spin chains. *Phys. Rev. Lett.*, 112:217204, May 2014.
5. J. Eisert, M. Friesdorf, and C. Gogolin. Quantum many-body systems out of equilibrium. *Nature Physics*, 11(2):124–130, feb 2015.
6. Pedro Ponte, Z. Papić, Fran çois Huveneers, and Dmitry A. Abanin. Many-body localization in periodically driven systems. *Phys. Rev. Lett.*, 114:140401, Apr 2015.
7. M. Azimi, L. Chotorlishvili, S. K. Mishra, S. Greschner, T. Vekua, and J. Berakdar. Helical multiferroics for electric field controlled quantum information processing. *Phys. Rev. B*, 89:024424, Jan 2014.
8. M. Azimi, M. Sekania, S. K. Mishra, L. Chotorlishvili, Z. Toklikishvili, and J. Berakdar. Pulse and quench induced dynamical phase transition in a chiral multi-ferroic spin chain. *Phys. Rev. B*, 94:064423, Aug 2016.
9. I. Medina, S. V. Moreira, and F. L. Semião. Quantum versus classical transport of energy in coupled two-level systems. *Phys. Rev. A*, 103:052216, May 2021.
10. Elliott H. Lieb and Derek W. Robinson. The finite group velocity of quantum spin systems. *Communications in Mathematical Physics*, 28(3):251–257, Sep 1972.
11. Anatoli Iwanowitsch Larkin and Yuriï N. Ovchinnikov. Quasiclassical method in the theory of superconductivity. *Journal of Experimental and Theoretical Physics*, 28(6):1200, jun 1969.
12. Juan Maldacena, Stephen H. Shenker, and Douglas Stanford. A bound on chaos. *Journal of High Energy Physics*, 2016(8):106, Aug 2016.
13. Daniel A. Roberts, Douglas Stanford, and Leonard Susskind. Localized shocks. *Journal of High Energy Physics*, 2015(3):51, Mar 2015.
14. Eiki Iyoda and Takahiro Sagawa. Scrambling of quantum information in quantum many-body systems. *Phys. Rev. A*, 97:042330, Apr 2018.
15. Adrian Chapman and Akimasa Miyake. Classical simulation of quantum circuits by dynamical localization: Analytic results for pauli-observable scrambling in time-dependent disorder. *Phys. Rev. A*, 98:012309, Jul 2018.
16. Brian Swingle and Debanjan Chowdhury. Slow scrambling in disordered quantum systems. *Phys. Rev. B*, 95:060201, Feb 2017.
17. Markus J. Klug, Mathias S. Scheurer, and Jörg Schmalian. Hierarchy of information scrambling, thermalization, and hydrodynamic flow in graphene. *Phys. Rev. B*, 98:045102, Jul 2018.
18. A. del Campo, J. Molina-Vilaplana, and J. Sonner. Scrambling the spectral form factor: Unitarity constraints and exact results. *Phys. Rev. D*, 95:126008, Jun 2017.
19. Michele Campisi and John Goold. Thermodynamics of quantum information scrambling. *Phys. Rev. E*, 95:062127, Jun 2017.
20. Sa šo Grozdanov, Koenraad Schalm, and Vincenzo Scopelliti. Black hole scrambling from hydrodynamics. *Phys. Rev. Lett.*, 120:231601, Jun 2018.
21. Aavishkar A. Patel, Debanjan Chowdhury, Subir Sachdev, and Brian Swingle. Quantum butterfly effect in weakly interacting diffusive metals. *Phys. Rev. X*, 7:031047, Sep 2017.
22. Vedika Khemani, Ashvin Vishwanath, and David A. Huse. Operator spreading and the emergence of dissipative hydrodynamics under unitary evolution with conservation laws. *Phys. Rev. X*, 8:031057, Sep 2018.
23. Tibor Rakovszky, Frank Pollmann, and C. W. von Keyserlingk. Diffusive hydrodynamics of out-of-time-ordered correlators with charge conservation. *Phys. Rev. X*, 8:031058, Sep 2018.
24. S. V. Syzranov, A. V. Gorshkov, and V. Galitski. Out-of-time-order correlators in finite open systems. *Phys. Rev. B*, 97:161114, Apr 2018.
25. Pavan Hosur, Xiao-Liang Qi, Daniel A. Roberts, and Beni Yoshida. Chaos in quantum channels. *Journal of High Energy Physics*, 2016(2):4, Feb 2016.
26. Nicole Yunger Halpern. Jarzynski-like equality for the out-of-time-ordered correlator. *Phys. Rev. A*, 95:012120, Jan 2017.
27. Eman Hamza, Robert Sims, and Günter Stolz. Dynamical localization in disordered quantum spin systems. *Communications in Mathematical Physics*, 315(1):215–239, Oct 2012.
28. Clément Hainaut, Ping Fang, Adam Rançon, Jean-François Clément, Pascal Szriftgiser, Jean-Claude Garreau, Chushun Tian, and Radu Chicireanu. Experimental observation of a time-driven phase transition in quantum chaos. *Physical review letters*, 121(13):134101, 2018.
29. A K Naik, M S Hanay, W K Hiebert, X L Feng, and M L Roukes. Towards single-molecule nanomechanical mass spectrometry. *Nature Nanotechnology*, 4(7):445, jul 2009.
30. A D O Connell, M Hofheinz, M Ansmann, Radoslaw C Bialczak, M Lenander, Erik Lucero, M Neeley, D Sank, H Wang, M Weides, J Wenner, John M Martinis, and A N Cleland. Quantum ground state and single-phonon control of a mechanical resonator. *Nature*, 464(7289):697, 2010.
31. T P Mayer Alegre, J Chan, M Eichenfield, M Winger, Q Lin, J T Hill, D E Chang, and O Painter. Electromagnetically induced transparency and slow light with optomechanics. *Nature*, 472(7341):69, 2011.

32. K. Stannigel, P. Rabl, A. S. Sørensen, P. Zoller, and M. D. Lukin. Optomechanical transducers for long-distance quantum communication. *Phys. Rev. Lett.*, 105(22):220501, 2010.
33. Amir H Safavi-Naeini and Oskar Painter. Proposal for an optomechanical traveling wave phonon–photon translator. *New Journal of Physics*, 13(1):013017, 2011.
34. Stephan Camerer, Maria Korppi, Andreas Jöckel, David Hunger, Theodor W. Hänsch, and Philipp Treutlein. Realization of an optomechanical interface between ultracold atoms and a membrane. *Phys. Rev. Lett.*, 107(22):223001, 2011.
35. Matt Eichenfield, Jasper Chan, Ryan M. Camacho, Kerry J. Vahala, and Oskar Painter. Optomechanical crystals. *Nature*, 462(7269):78–82, nov 2009.
36. Amir H. Safavi-Naeini, Jasper Chan, Jeff T. Hill, Thiago P. Mayer Alegre, Alex Krause, and Oskar Painter. Observation of quantum motion of a nanomechanical resonator. *Phys. Rev. Lett.*, 108(3):033602, 2012.
37. Nathan Brahms, Thierry Botter, Sydney Schreppler, Daniel W C Brooks, and Dan M. Stamper-Kurn. Optical detection of the quantization of collective atomic motion. *Phys. Rev. Lett.*, 108(13):133601, 2012.
38. A. Nunnenkamp, K. Børkje, and S. M. Girvin. Cooling in the single-photon strong-coupling regime of cavity optomechanics. *Phys. Rev. A*, 85(5):051803(R), 2012.
39. Farid Ya Khalili, Haixing Miao, Huan Yang, Amir H. Safavi-Naeini, Oskar Painter, and Yanbei Chen. Quantum back-action in measurements of zero-point mechanical oscillations. *Phys. Rev. A*, 86(3):033602, 2012.
40. Charles P. Meaney, Ross H. McKenzie, and G. J. Milburn. Quantum entanglement between a nonlinear nanomechanical resonator and a microwave field. *Phys. Rev. E*, 83(5):056202, 2011.
41. J. Atalaya, A. Isacsson, and M. I. Dykman. Diffusion-induced dephasing in nanomechanical resonators. *Phys. Rev. B*, 83(4):045419, 2011.
42. P. Rabl. Cooling of mechanical motion with a two-level system: The high-temperature regime. *Phys. Rev. B*, 82(16):165320, 2010.
43. Levan Chotorlishvili, Zaza Toklikishvili, and Jamal Berakdar. Thermal entanglement and efficiency of the quantum otto cycle for the su (1, 1) tavis–cummings system. *Journal of Physics A: Mathematical and Theoretical*, 44(16):165303, 2011.
44. S. V. Prants. A group-theoretical approach to study atomic motion in a laser field. *J. Phys. A*, 44(26):265101, jul 2011.
45. Max Ludwig, K. Hammerer, and Florian Marquardt. Entanglement of mechanical oscillators coupled to a nonequilibrium environment. *Phys. Rev. A*, 82(1):012333, 2010.
46. Thomas L. Schmidt, Kjetil Børkje, Christoph Bruder, and Björn Trauzettel. Detection of qubit-oscillator entanglement in nanoelectromechanical systems. *Phys. Rev. Lett.*, 104(17):177205, 2010.
47. R. B. Karabalin, M. C. Cross, and M. L. Roukes. Nonlinear dynamics and chaos in two coupled nanomechanical resonators. *Phys. Rev. B*, 79(16):165309, 2009.
48. L Chotorlishvili, A Ugulava, G Mchedlishvili, A Komnik, S Wimberger, and J Berakdar. Nonlinear dynamics of two coupled nano-electromechanical resonators. *Journal of Physics B: Atomic, Molecular and Optical Physics*, 44(21):215402, oct 2011.
49. S. N. Shevchenko, A. N. Omelyanchouk, and E. Il'ichev. Multiphoton transitions in Josephson-junction qubits (Review Article). *Low Temperature Physics*, 38(4):283–300, 2012.
50. Yu Xi Liu, Adam Miranowicz, Y. B. Gao, Jiří Bajer, C. P. Sun, and Franco Nori. Qubit-induced phonon blockade as a signature of quantum behavior in nanomechanical resonators. *Phys. Rev. A*, 82(3):032101, 2010.
51. S.N. Shevchenko, S. Ashhab, and Franco Nori. Landau–Zener–Stückelberg interferometry. *Physics Reports*, 492(1):1–30, jul 2010.
52. David Zueco, Georg M. Reuther, Sigmund Kohler, and Peter Hänggi. Qubit-oscillator dynamics in the dispersive regime: Analytical theory beyond the rotating-wave approximation. *Phys. Rev. A*, 80(3):033846, 2009.
53. Guy Z. Cohen and Massimiliano Di Ventra. Reading, writing, and squeezing the entangled states of two nanomechanical resonators coupled to a SQUID. *Phys. Rev. B*, 87(1):014513, 2013.
54. P. Rabl, P. Cappellaro, M. V. Gurudev Dutt, L. Jiang, J. R. Maze, and M. D. Lukin. Strong magnetic coupling between an electronic spin qubit and a mechanical resonator. *Phys. Rev. B*, 79(4):041302(R), 2009.
55. Li Gong Zhou, L. F. Wei, Ming Gao, and Xiang Bin Wang. Strong coupling between two distant electronic spins via a nanomechanical resonator. *Phys. Rev. A*, 81(4):042323, 2010.
56. L. Chotorlishvili, D. Sander, A. Sukhov, V. Dugaev, V. R. Vieira, A. Komnik, and J. Berakdar. Entanglement between nitrogen vacancy spins in diamond controlled by a nanomechanical resonator. *Phys. Rev. B*, 88(8):085201, 2013.
57. R. B. Karabalin, M. C. Cross, and M. L. Roukes. Nonlinear dynamics and chaos in two coupled nanomechanical resonators. *Phys. Rev. B*, 79:165309, Apr 2009.
58. A. K. Singh, L. Chotorlishvili, S. Srivastava, I. Tralle, Z. Toklikishvili, J. Berakdar, and S. K. Mishra. Generation of coherence in an exactly solvable nonlinear nanomechanical system. *Phys. Rev. B*, 101:104311, Mar 2020.
59. Dimitrios Maroulakos, Levan Chotorlishvili, Dominik Schulz, and Jamal Berakdar. Local and non-local invasive measurements on two quantum spins coupled via nanomechanical oscillations. *Symmetry*, 12(7):1078, 2020.
60. H. Y. Chen, E. R. MacQuarrie, and G. D. Fuchs. Orbital state manipulation of a diamond nitrogen-

- vacancy center using a mechanical resonator. *Phys. Rev. Lett.*, 120:167401, Apr 2018.
61. Gautam Kamalakar Naik, Rajeev Singh, and Sunil Kumar Mishra. Controlled generation of genuine multipartite entanglement in floquet ising spin models. *Phys. Rev. A*, 99:032321, Mar 2019.
 62. Tzu-Chieh Wei and Paul M. Goldbart. Geometric measure of entanglement and applications to bipartite and multipartite quantum states. *Phys. Rev. A*, 68:042307, Oct 2003.
 63. M. Blasone, F. Dell'Anno, S. De Siena, and F. Illuminati. Hierarchies of geometric entanglement. *Phys. Rev. A*, 77:062304, Jun 2008.
 64. Charles Kittel and Ching-yao Fong. *Quantum theory of solids*, volume 5. Wiley New York, 1963.